Journal of Structural Geology 31 (2009) 1340–1349

Contents lists available at ScienceDirect

Journal of Structural Geology

journal homepage: www.elsevier.com/locate/jsg

Controls of folding on different scales in multilayered rocks

Susan H. Treagus [a,*], Raymond C. Fletcher [b]

[a] School of Earth, Atmospheric and Environmental Sciences, University of Manchester, Manchester M13 9PL, England, UK
[b] Centre for Physics of Geological Processes, University of Oslo, NO-0316 Oslo, Norway

ARTICLE INFO

Article history:
Received 2 February 2009
Received in revised form
22 July 2009
Accepted 31 July 2009
Available online 5 August 2009

Keywords:
Folding
Multilayers
Viscous media
Buckling instability
Major and minor folds

ABSTRACT

Folding at different scales is ubiquitous in orogenic belts, and small-scale folds are commonly used to constrain the geometry of larger-scale folds. Analyses of viscous multilayers of N equally-thick stiff layers show that the rate of fold amplification and the dominant wavelength to layer thickness increase with N. This suggests that large-scale multilayer folds would initiate earlier than small-scale minor folds in a single layer or a few layers. How then do the latter amplify at a faster rate than the former to become minor folds on the limbs of larger-scale folds?

To answer this question, analytical models of fold initiation in multilayers that contain stiff layers with different thicknesses and viscosities were studied. The models comprise five alternating stiff/soft viscous layers, with a thinner or thicker central stiff layer, in a soft confinement by either viscous half spaces or finite layers against rigid frictionless platens. One or two maxima may occur in the amplification rate – wavelength spectrum: if two, the stronger buckling instability may be either that of the multilayer or a single layer. Early initiation of single-layer folds in a central thin layer is favoured if the multilayer is narrowly confined, and if the layer is significantly stiffer than the adjacent stiff layers. Folds then develop on two scales, creating potential 'minor' and 'major' folds. In models with a thicker central layer, amplification rate decreases as the layer thickness increases. Unusually thick competent layers in a confined multilayer do not act as 'control units' that enhance folding; instead they impede folding.

1. Introduction

Folds are a ubiquitous feature of stratified rocks in orogenic belts, and are seen on many different scales. One long-held method used by structural geologists in the field is to use the asymmetry and vergence of small-scale folds to indicate the geometry of larger-scale folds (Fig. 1). In this paper, we address the question of why small-scale folds, sometimes termed minor or parasitic folds, initiate in multilayered rocks and are preserved in larger-scale folds in fold belts. It was shown in early analyses of folding in viscous media (Biot, 1961, 1965a; Ramberg, 1963, 1964) that a multilayer comprising numerous stiff layers would fold with a stronger amplification than a single stiff layer in the same host, and that the buckling instability increases with the number of stiff layers. This result has since been verified by many other theoretical and model studies (Johnson and Fletcher, 1994; Mühlhaus et al., 2002; Schmid and Podladchikov, 2006). A reasonable conclusion, therefore, might be that relatively large folds affecting numerous layers would fold more strongly than smaller folds affecting one or few layers. However, this is not borne out by field studies, and the minor–major fold rule referred to above and in Fig. 1. There would thus appear to be a paradox: how do small folds of one or two layers buckle with a strong enough instability to become the small-scale folds or 'minor' folds preserved around the larger-scale folds?

Part of the answer to this paradox might be that the differences in amplification between single and multilayer folds are not very great. Schmid and Podladchikov (2006) clarify differences between single and multilayer folding, presenting parameters such as dominant wavelength and amplification normalized to the single layer. They demonstrate that the strongest folding instability arises where alternating stiff and soft layers have equal thickness. This result is also inferred from Biot's (1961, 1965a, 1965b) analyses that treat multilayers as statistically anisotropic, as this is the arrangement with the maximum anisotropy. In the Schmid and Podladchikov (2006) model, with 10 stiff layers interlayered with 9 soft layers of the same thickness, bonded contacts, and a viscosity contrast of 25, the maximum amplification factor (q) of the multilayer folds, at their dominant wavelength to layer thickness value, L_d/T, is 1.6 times the single-layer q value. This quantity (q) occurs in a relation of the form

* Corresponding author.
E-mail address: susan.h.treagus@manchester.ac.uk (S.H. Treagus).

0191-8141/$ – see front matter © 2009 Elsevier Ltd. All rights reserved.
doi:10.1016/j.jsg.2009.07.009

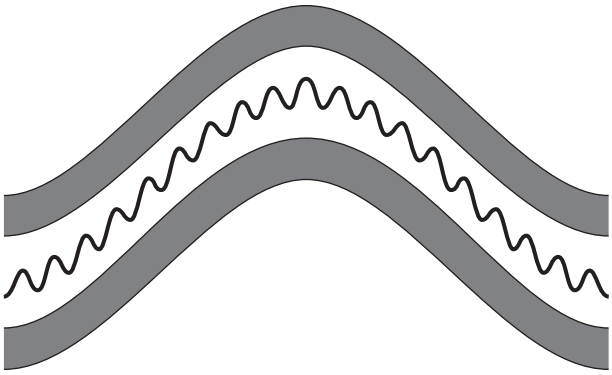

Fig. 1. Schematic illustration of 'minor' folds in a thin single layer within 'major' folds of a multilayer. A traditional field method in structural geology is to use the asymmetry and vergence of minor folds to indicate the presence of larger-scale major folds.

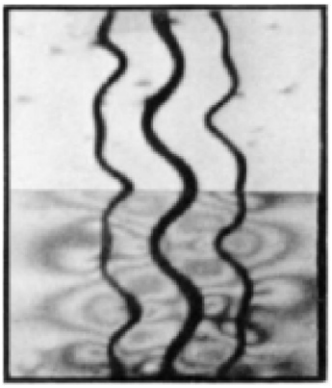

Fig. 2. An enlarged photoelastic analogue model from Currie et al. (1962, plate 2, fig. 5), showing folding on two scales. Three rubber layers, the central layer twice the thickness of the other two, in a gelatine matrix. Note folding on two scales in the thinner layer which is within the zone of contact strain of the thicker layers, but not vice versa.

$$\frac{1}{A_j}\frac{\mathrm{d}A_j}{\mathrm{d}_t} = q|\overline{D}_{xx}| \tag{1}$$

where A_j is one of a set of amplitudes comprising a multilayer eigenmode, q is the associated eigenvalue (e.g. see Johnson and Fletcher, 1994), t is time, and $\overline{D}_{xx} < 0$ is the basic-state rate of shortening. If q is such that an amplification of 10 occurs in a specified increment of shortening, a value that is 1.6 times as large will produce an amplification of ~40. In general, as in the present paper, the eigenmode with the largest q is of chief interest.

Johnson and Fletcher (1994, see figs 6.11 and 6.12) obtained much larger differences than this in amplification factor, q, for a multilayer comprising 9 stiff layers alternating with 8 soft layers, embedded in an infinite soft medium, where all the layers have free slip interfaces. Despite a viscosity ratio of only 10, this multilayer has $q_d \sim 6$ times that of the single layer. So clearly there are factors, here free interfacial slip, that have a much greater effect on buckling than just the number of stiff layers in an alternating stiff–soft multilayer with layers of equal thickness.

Johnson and Fletcher (1994) obtain numerical solutions for selective amplification in low-amplitude folding for many examples of multilayers with different configurations of stiff and soft layers and embedding medium. They demonstrate that the strength of the folding instability generally increases with the following: the number of stiff layers involved; increasing viscosity ratios between the stiff and soft layers; where a multilayer is in a soft 'infinite' embedding medium, rather than between rigid, frictionless platens; and where there is free slip between layers, rather than bonded contacts. This last difference is much more significant for folding of a multilayer than for folding of a single layer.

Stratified rocks will rarely be as regular as these theoretical multilayer models, however. In a ground-breaking paper, Currie et al. (1962) considered folding of sedimentary strata, and introduced the term *structural lithic unit* (SLU) to distinguish packets of multilayered rock that fold discretely and are self-confined within a larger layered system. Typically, the SLU shows maximum folding in the centre, either a single layer or a group of layers that the authors termed the *dominant member*, and the SLU is bounded by softer layers above and below. Such an arrangement will form the basis of one set of analytical models considered in this paper.

In apparent conflict with the SLU concept, Price and Cosgrove (1990, p. 321) suggest that folding in multilayers is generated from *control units*, usually anomalously thick stiff layers in the multilayer, which effectively fold as single layers, and dominate the folding. We will test the theoretical validity of this concept.

In their classic analogue experiments, Currie et al. (1962) used stiff layers of rubber of varying thickness, in softer, photoelastic gelatine, to illustrate the change from quasi single layer to in-phase multilayer folding, as the spacing of the rubber layers decreased. Fig. 2 is one example. The photoelastic fringes demonstrate what Ramberg (1962) called the *zone of contact strain* created in the adjacent soft layers or medium by a stiff folded layer; he found the zone to extend to approximately the initial fold wavelength (L_d) to either side of the folding layer or layers. In Fig. 2, which is particularly relevant to this paper, the model comprises three stiff layers, the central layer double the thickness of the other two. The thick layer folded with a large wavelength, clearly influencing the folding of the thin layers a distance of about half its wavelength away, within its zone of contact strain. However, the thick layer is outside their zones of contact strain for folding at a second, much smaller wavelength. Thus the thick layer folds as a simple wave, whereas the thinner layers show *two different wavelengths*, as these layers fold approximately as single layers, but are also incorporated into the longer wavelength multilayer folding. Although showing folding of elastic materials, Fig. 2 demonstrates aspects of multilayer folding that we will investigate further in this paper, through analytical modelling of folding instability in viscous multilayers.

Ramberg (1964) investigated fold processes in multilayers that comprised combinations of thin and thick layers and varied viscosity contrasts. He introduced the concept of different *orders of folding*, the first-order being the largest scale, and discussed related processes such as the modification of small, or parasitic, folds around larger folds, minor and major fold relationships, and fold vergence (Fig. 1). All these are now standard text-book methods for field geologists. In this paper, we prefer the term *scales of folding*, rather than *orders*, because of possible confusion between orders of scale, noted above, and order of initiation or growth, which might indicate the opposite. In this seminal paper, Ramberg (1964) showed that in a non-regular multilayer, the stiffest layers will fold most strongly, and that several stiff layers will fold more strongly than one.

Johnson and Fletcher (1994) treat folding in sequences of layers of different thicknesses that might simulate realistic stratigraphy. Their models also show folding on two scales, with almost the same amplification factor. The finite-amplitude result would be trains of smaller and larger folds that grew at similar rates.

We return to the rule of field structural geology that opened this paper: that the asymmetry of small or parasitic folds can be used to indicate larger-scale folding. When considered in conjunction with

theoretical modelling of multilayer folding reviewed above, we find a paradox. Theory and modelling show that the folding instability in a multilayer *increases* with the number of stiff layers, suggesting that folding of numerous layers would be stronger than folding of single layers on a smaller scale. However, in stratified rocks in nature, for the field rule of minor and major folding to work as it does, the *smallest folds must initiate first*, probably in one or a few layers, and, in order to be preserved on limbs of larger folds, must *grow faster* than the larger folds that involve more layers. Carrying this argument to its conclusion, the largest-scale folding, affecting perhaps the whole stratigraphic succession, will be the slowest to amplify and grow. Such a conclusion would appear to run counter to theoretical studies reviewed above that suggest that the larger the number of stiff layers, the stronger the folding instability.

A resolution of this paradox is offered by Frehner and Schmalholz (2006), who simulate, in numerical FEM models, the development of small 'parasitic folds' in thin multilayers sandwiched between thick layers, 50 times as thick as the thin stiff layers in the multilayer, but with the same viscosity. The large folds developed from a prescribed sinusoidal perturbation, whereas the small folds, with 'wavelength' ~1/50th that of the thick layer folds, developed from random interfacial perturbations, and are less regular. The small folds will always appear in the hinge regions of the larger folds, and provided folding of the thick layers does not re-orient the thin layers away from the direction of shortening prior to adequate fold amplification, they will develop over the full span of the large folds. Frehner and Schmalholz (2006) most successfully obtain small folds over the full span by reducing the ratio of initial amplitude to layer thickness (A/H) of the thick-layer sinusoidal perturbation, while retaining the scale of random perturbations for the thin layers. They assert that such a reduction in initial perturbation amplitude with layer thickness may be a common feature of stratified rock sequences, where initial amplitudes are sedimentary structures such as wave ripples of a characteristic size, causing the initial A/H ratio to be much larger in thin than in thick layers. Based on these assumptions, the numerical models of Frehner and Schmalholz (2006) demonstrate this as one mechanism for the growth of small 'parasitic' folds around larger 'major' folds. However, their parasitic folds are mostly in thin multilayers, rather than a single layer, and are not regular sinusoidal perturbations, so we do not think they provide the best answer for the two scales of folding idealised in Fig. 1, the focus for this paper.

Here, we are interested in conditions where small single-layer folds can successfully grow within a folding multilayer, and where the smaller folds might outpace the larger multilayer folds. We will analyse multilayer folding on different scales, and investigate variables such as multilayer configuration and confinement, layer thickness and viscosity ratios, to determine which factors will overturn the simple conclusion from early analytical models, that multilayers generally fold more strongly than single layers.

2. Analysis of multilayer folding at different scales

In the preceding review, it was shown that multilayers comprising alternating stiff and soft layers, confined between soft viscous half spaces, will have the maximum buckling instability where the layers have the same thickness. The strength of fold amplification increases with the number of layers, always exceeding that of a single layer. What we will investigate here is folding in multilayers that are not so regular, and not always confined by semi-infinite half spaces. Our models comprise three stiff layers of varying thickness, separated by soft layers, and in a soft confinement that is either a viscous half space or a finite layer against rigid frictionless platens (RFPs) (Fig. 3). The latter is a model for a structural lithic unit (SLU) after Currie et al. (1962), that we call

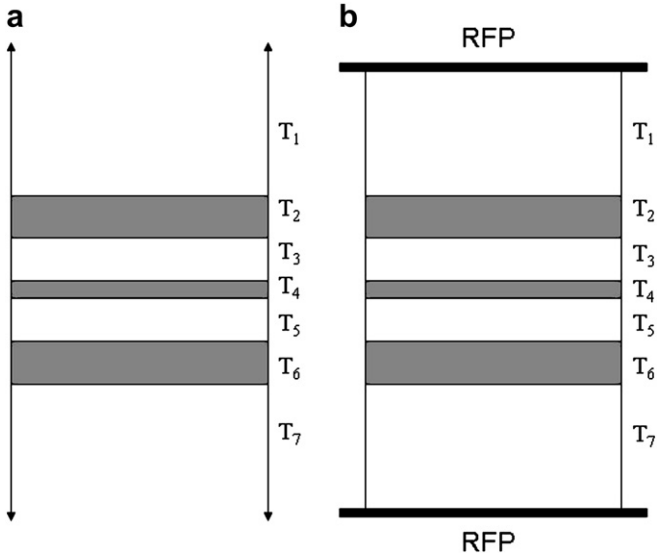

Fig. 3. Design of analytical models. (a) Model 1, a 5-layer multilayer confined in a viscous half space (quasi-infinite). (b) Model 2, a 5-layer multilayer with a finite confining layer against rigid frictionless platens (RFP), which makes a 7-layer 'structural lithic unit', termed SLU7. Stiff layers (thicknesses T_2, T_4, T_6) are shaded. Interlayers (T_3, T_5) and outer confining layers (T_1, T_7) are soft media, unshaded. Layers T_2–T_6 all have the same thickness, whereas T_4 is thinner. Models 3 and 4 are designed similarly, but with T_4 thicker than the other layers (defined in the text).

SLU7 because it comprises 7 layers in total (Fig. 3b). Additionally, we restrict this modelling to welded interfaces, and Newtonian viscous layers with two or three different viscosities.

2.1. The analytical method

The analysis only concerns wavelength selection in low-amplitude folding, a subject first introduced into the literature of structural geology by Ramberg (e.g. 1962) and Biot (1961). A detailed development of the relevant analysis, together with comprehensive reference to previous work, as applied to folding of purely viscous, homogeneous layers at small enough bulk rates of shortening that elastic effects are negligible, is given in Johnson and Fletcher (1994). In essence, as a volume of layered rock, so modelled, is subjected to an arbitrary history of homogeneous bulk, or basic-state, shortening, linearly independent components of the interfacial perturbation, present on all layer surfaces are amplified. As interfaces reach slopes of ~5–15°, linearly independent growth of components breaks down, and the fold structure, in terms of fold hinge positions, fold arclengths, and layer thicknesses, is locked in. The analysis, carried out to first-order in interfacial slope, is a thick-plate analysis applied to multilayer configurations.

Representing the amplitudes, at a given wavelength L, of the six deformable interfaces of our three stiff layer multilayer as column vectors, an arbitrary form of the multilayer can be decomposed into these two forms

$$\begin{bmatrix} A_1 \\ A_2 \\ A_3 \\ A_4 \\ A_5 \\ A_6 \end{bmatrix} = \frac{1}{2}\begin{bmatrix} A_1 + A_6 \\ A_2 + A_5 \\ A_3 + A_4 \\ A_3 + A_4 \\ A_2 + A_5 \\ A_1 + A_6 \end{bmatrix} + \frac{1}{2}\begin{bmatrix} A_1 - A_6 \\ A_2 - A_5 \\ A_3 - A_4 \\ -(A_3 - A_4) \\ -(A_2 - A_5) \\ -(A_1 - A_6) \end{bmatrix} \quad (2)$$

Here, A_1 and A_2 are the amplitudes of the upper stiff layer, whose thickness is designated T_2; A_3 and A_4 are the amplitudes of the central stiff layer, whose thickness is designated T_4; and

A_5 and A_6 are the amplitudes of the lower stiff layer, also with thickness T_2. Since the thicknesses and viscosities of the layers in the multilayers considered here are symmetric about the central stiff layer, these two forms do not interact – i.e. they are linearly independent, in the case of uniform layer-parallel shortening. That is, by symmetry of the configuration about the central layer, the central layer must either have a pure fold form or a pure pinch-and-swell form in any of the six eigenmodes, and each eigenmode is linearly independent of the others. Here, we will only consider the first form, in which the central stiff layer has a pure fold form. For simplicity we may write the column of amplitudes for this form as

$$\begin{bmatrix} A_1 \\ A_2 \\ A_3 \\ A_3 \\ A_2 \\ A_1 \end{bmatrix} \tag{3}$$

The evolution equations for the amplitudes, to first-order in slopes, λA_j, where $\lambda = 2\pi/L$ is the wavenumber, are of the form

$$\begin{aligned} \frac{1}{|\overline{D}_{xx}|}\frac{dA_1}{dt} &= q_{11}A_1 + q_{12}A_2 + q_{13}A_3 \\ \frac{1}{|\overline{D}_{xx}|}\frac{dA_2}{dt} &= q_{21}A_1 + q_{22}A_2 + q_{23}A_3 \\ \frac{1}{|\overline{D}_{xx}|}\frac{dA_3}{dt} &= q_{31}A_1 + q_{32}A_2 + q_{33}A_3 \end{aligned} \tag{4}$$

In the approximation that the coefficients q_{ij} are constant, which will be adopted here, the set of linear differential equations has three linearly independent solutions, or eigenmodes, and the general solution may be written as a sum of the eigenmodes

$$\begin{bmatrix} A_1(|\overline{D}_{xx}|t) \\ A_2(|\overline{D}_{xx}|t) \\ A_3(|\overline{D}_{xx}|t) \end{bmatrix} = \begin{bmatrix} A_1^{(I)}(0) \\ A_2^{(I)}(0) \\ A_3^{(I)}(0) \end{bmatrix} e^{q_I|\overline{D}_{xx}|t} + \begin{bmatrix} A_1^{(II)}(0) \\ A_2^{(II)}(0) \\ A_3^{(II)}(0) \end{bmatrix} e^{q_{II}|\overline{D}_{xx}|t} + \begin{bmatrix} A_1^{(III)}(0) \\ A_2^{(III)}(0) \\ A_3^{(III)}(0) \end{bmatrix} e^{q_{III}|\overline{D}_{xx}|t} \tag{5}$$

where each column on the right-hand side is proportional to an eigenvector, of which there are three, and q_I, q_{II} and q_{III} are the corresponding eigenvalues. Note that this implies that a set of initial amplitudes can be allocated to the initial amplitudes of the three eigenmodes, so that

$$A_j(0) = A_j^{(I)}(0) + A_j^{(II)}(0) + A_j^{(III)}(0) \tag{6}$$

$j = 1,2,3$.

Since the coefficients are functions of the wavelength, L, as well as the thicknesses and viscosities of the layers, there is a solution of this form for each L. Eigenvectors and eigenvalues of the matrix X are determined here using the subroutine eig(X) in Matlab©.

The bulk strain dependence in (5) is expressed as commonly done as though the magnitude of the bulk rate of shortening $|\overline{D}_{xx}|$were constant in time. In this case, the stretch equivalent to the bulk shortening, but expressed as the complementary layer-normal bulk stretching, is $S = \exp(|\overline{D}_{xx}|t) \geq 1$. For an arbitrary history of bulk shortening, we may replace the forms shown by $S^{q_I}, S^{q_{II}}, S^{q_{III}}$, where S is now the path-independent, or shortening history independent, cumulative bulk extension. This result only applies when the layers are linear viscous media.

In general, at any wavelength, one of the eigenvalues will be positive and greater than the other two, and with increasing $|\overline{D}_{xx}|t$, its contribution to the solution will outstrip the others. We therefore principally characterize the solution in terms of the value of this maximum eigenvalue, denoted simply as

$$q = \max[q_I, q_{II}, q_{III}] \tag{7}$$

where all eigenvalues are taken as functions of L/T_2, where T_2 is the thickness of either of the outer stiff layers. We speak of the function $q(L/T_2)$ as the maximum eigenvalue spectrum.

The spectrum of this maximum eigenvalue will show one or two peaks, at different L/T_2, and, as with the definition of a dominant wavelength for folding of a single layer, we may define a dominant wavelength to thickness ratio, L_d/T_2 and an associated eigenvalue, q_d. If there are two peaks, the lower pair will be designated $(L_d/T_2)'$ and q_d'. When there are two peaks, cases in which q_d and q_d' are comparable in magnitude will be of special interest. q is described as the *amplification factor* by Johnson and Fletcher (1994, p. 205), and q_d is accordingly a measure of the amplification of the dominant wavelength, L_d.

The eigenvectors are, of course, of equal interest, since they describe the form of the multilayer structure that emerges as selective amplification continues, but we will not devote space in the paper to a detailed account of their numerical forms and variation. The most salient fact is that the eigenvectors – i.e. the relative magnitudes of the three amplitudes – associated with the locally dominant modes will be of one of three types. In all cases, one dominant mode has amplitudes of nearly equal magnitude. We informally term this the multilayer mode (ML). The other mode, locally dominant as a peak in the q, L/T_2 – spectrum, corresponds to a constrained single-layer mode (SL). Indeed, this is still a multilayer mode, and L_d and q_d for this mode may differ markedly from their values for a single layer embedded in an infinite medium. If the central stiff layer is thinner than the other stiff layers, this mode will correspond to an amplitude A_3 relatively much larger than that of the other surfaces. If the central layer is thicker than the outer stiff layers, an SL mode will express itself as relatively large and sub-equal amplitudes of the outer stiff layers and low amplitude of the inner stiff layer. Very approximately, these modes may be characterized as

$$\begin{aligned} \begin{bmatrix} A_1 \\ A_2 \\ A_3 \end{bmatrix}^{(ML)} &\sim \begin{bmatrix} 1 \\ 1 \\ 1 \end{bmatrix} \\ \begin{bmatrix} A_1 \\ A_2 \\ A_3 \end{bmatrix}^{(SL)} &\sim \begin{bmatrix} 0 \\ 0 \\ 1 \end{bmatrix} \\ \begin{bmatrix} A_1 \\ A_2 \\ A_3 \end{bmatrix}^{(SL)'} &\sim \begin{bmatrix} 1 \\ 1 \\ 0 \end{bmatrix} \end{aligned} \tag{8}$$

We emphasize that all modes are multilayer modes, and it is only exceptionally that a single layer can be so thin and sufficiently separated from other stiff layers that its behaviour is quantitatively close to that of an isolated single layer. As we will show, the SL mode is favoured if the viscosity of the layer is significantly greater than the other stiff layers.

To demonstrate the adequacy of the approximation, we plot both the maximum eigenvalue and the geometric quantity

$$G = \frac{A_1 + A_2}{2A_3} \tag{9}$$

as derived from the eigenvector associated with the maximum eigenvalue. This is the ratio of the mean amplitude of the outer stiff layer to the amplitude of the central stiff layer. The example in Fig. 4

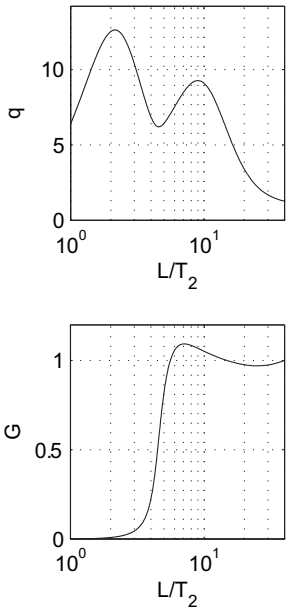

Fig. 4. q and G for one model (Fig. 3b design), with $T_1/T_2 = 4$, $T_3/T_2 = 1$ and $T_4/T_2 = 0.2$. The central stiff layer is twice as stiff as the outer stiff layers and their viscosity is 20 times that of the soft interlayers. The larger SL mode has a dominant wavelength $L_d/T_2 = 9$ or $L_d/T_4 = 45$; the ML mode has $L_d/T_2 = 11.9$ or $L_d/T_4 = 59.3$. Hence ~5 wavelengths of the dominant SL mode occupy every wavelength of the dominant ML mode.

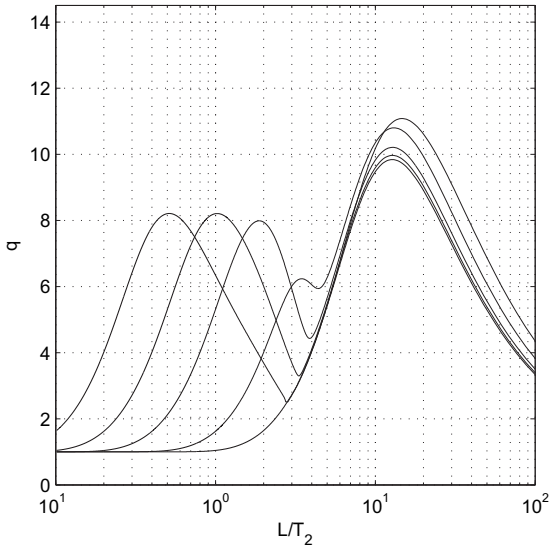

Fig. 5. Results for Model 1A series, a 5-layer multilayer with central thinner layer bound by a viscous half space. Viscosity ratio = 20. q spectra for different wavelengths, L (normalized to the outer stiff layer, T_2), where q is the dimensionless amplification factor; peaks signify dominant wavelengths (q_d, L_d) for single or multilayer folding. Curves are drawn for thin layer values, T_4/T_2, of 1.0, 0.5, 0.2, 0.1 and 0.05. The 1.0 curve has a single peak, the maximum for this series. The 0.5 curve has a shoulder, and the 0.2, 0.1 and 0.05 curves have two peaks, right indicating a stronger ML mode and left a weaker SL mode.

shows the clear distinction between the region about the long-wavelength ML peak, for which $G \approx 1$, and the region about the peak at small L/T_2, the central layer SL peak, at which $G \approx 0$. If the central layer is thicker than the outer stiff layers, the SL mode will have $G >> 1$, and the quantity $1/G$ might be a better diagnostic.

3. Models of multilayer folding on different scales: results

3.1. Model 1: 5-layer multilayer with central thin layer in viscous half space

Model 1A comprises three stiff layers with thicknesses T_2, T_4 and T_6, separated by soft layers (T_3 and T_5), and bounded by viscous half space (Fig. 3a). The stiff/soft viscosity ratio is 20. All layer thicknesses (T_2, T_3, T_5, T_6) are the same, except for the central stiff layer (T_4), which is thinner, with values $T_4/T_2 = 1$, 0.5, 0.2, 0.1 and 0.05. Fig. 5 shows q spectra for the series of models, with wavelengths scaled to T_2. The maximum ($q_d = 11$, $L_d/T_2 = 14.8$) is for the multilayer (ML) mode of folding where $T_4/T_2 = 1$. Nearby peaks with L_d/T_2 of ~12–15 are all for the ML mode, for decreasing values of T_4/T_2. The range is for three equal layers spaced at unit distance apart, to two stiff layers spaced at ~2 units apart. This limit is closely approached for $T_4/T_2 = 0.1$, with the reduction to $T_4/T_2 = 0.05$ having little additional effect. Note that there are two peaks of identical height and shape at much smaller values of L_d/T_2, which are the single-layer (SL) modes for $T_4/T_2 = 0.05$ and 0.1. If q were plotted versus L/T_4, they would coincide, giving SL $q_d \sim 8.2$ and $L_d/T_4 \sim 10.2$. The experiments shown in Fig. 5 show that the SL peak will never be larger than the ML peak. If we want such a result, an additional rheological, effect must be introduced.

Model 1B is a series of experiments with the same variables as Model 1A, except that we double the stiffness of the central thin layer, so that $\eta_4/\eta_3 = 40$, while $\eta_2/\eta_3 = 20$. As before, $T_3/T_2 = 1$ and $T_4/T_2 = 0.05$, 0.1, 0.2, 0.5 and 1. Fig. 6 shows that the maximum folding amplification is again seen where $T_4/T_2 = 1$, but now $q_d = 14.2$, and $L_d/T_2 = 16$. Stiffening the central layer therefore enhances the ML mode, as seen by comparing Fig. 6 with Fig. 5. However, what is particularly apparent in Fig. 6 is that even the strongest ML instability (for $T_4/T_2 = 1$), is only marginally greater than the strongest SL instability for the thin central layer (where $T_4/T_2 = 0.05$ and 0.1). When $T_4/T_2 \leq 0.2$, the SL mode of the central layer has the larger q_d than the ML mode, and so in these experiments, small folds in the central thin layer will grow more strongly

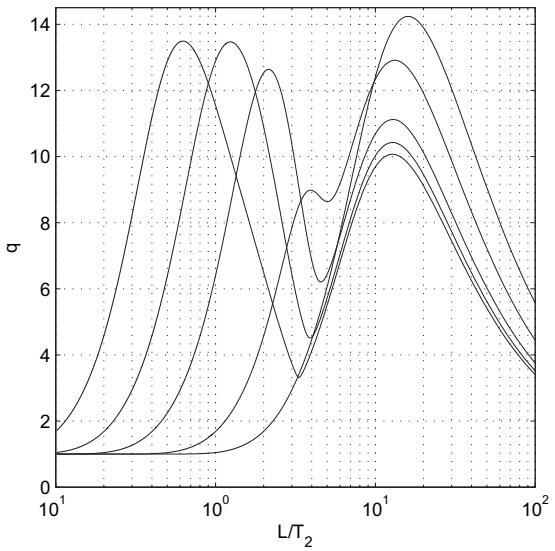

Fig. 6. Results for Model 1B series, a 5-layer multilayer with central thinner and stiffer layer bound by a viscous half space. Viscosity ratios 20 and 40. q spectra for different wavelengths, L (normalized to the outer stiff layer, T_2), where q is the dimensionless amplification factor; peaks signify dominant wavelengths (q_d, L_d) for single or multilayer folding. Curves are drawn for the thin layer values, T_4/T_2, of 1.0, 0.5, 0.2, 0.1 and 0.05. The 1.0 curve has a single peak, the maximum for this series. The 0.5 curve has a shoulder, and the 0.2, 0.1 and 0.05 curves have two peaks, right indicating a weaker ML mode and left a stronger SL mode, differing from Fig. 5.

that larger folds in the whole multilayer, and have the potential to become 'parasitic' folds. For example, for $T_4/T_2 = 0.1$, we have SL $q_d \sim 13.5$ versus the ML $q_d \sim 10$, a modest but important difference. The respective amplifications for 10% layer shortening are 3.9 versus 2.7, at 20% shortening, 15 versus 7.4, and at 30% shortening, 57 versus 20. These values are approximate, obtained from $\exp(q_d D_{xx} t)$ and do not take into account layer-parallel shortening, as in Sherwin and Chapple (1968).

3.2. Model 2: 5-layer multilayer with central thin layer and finite soft bounding layers against rigid frictionless platens: SLU7 model type

In this first SLU7 model, we take $T_1/T_2 = 3$: i.e. the bounding soft layers are just three times the thickness of the outer stiff layers (Fig. 3b). Otherwise, Model 2 uses the same variables as Model 1, in order to examine the differences between multilayers embedded within a viscous half space and those with a finite narrower confinement.

Model 2A comprises three stiff layers with thicknesses T_2, T_4 and T_6, separated by soft layers (T_3 and T_5). Layer thicknesses (T_2, T_3, T_5, T_6) are equal, except for the central stiff layer (T_4), which is thinner, with values $T_4/T_2 = 0.05$, 0.1, 0.2, 0.5 and 1. This multilayer is bounded by soft layers of thicknesses $T_1 = T_7$, where $T_1/T_2 = 3$. The stiff/soft viscosity ratio is 20. The results in Fig. 7 show that the thin central layer can now show a single-layer mode with larger q_d than the multilayer mode. The initial thinning of the central layer to 0.5 leads to a slightly larger ML q_d than the $T_4/T_2 = 1$ case, which is always the maximum for the comparable viscous half space model (Model 1A). For $T_4/T_2 = 0.2$, 0.1, and 0.05, the SL mode has a slightly larger q_d than the ML mode, but in terms of finite fold growth, small single-layer folds would probably grow at approximately the same rate as larger multilayer folds. This is a different result from Model 1A (Fig. 5), with the same layers but in a viscous half space.

Model 2B is essentially the same as Model 2A, except that the viscosity of the thinner central layer is doubled, so that $\eta_4/\eta_3 = 40$, while $\eta_2/\eta_3 = 20$. It is directly comparable to Model 1B, except for the finite soft confining layers against platens. Now, a quite

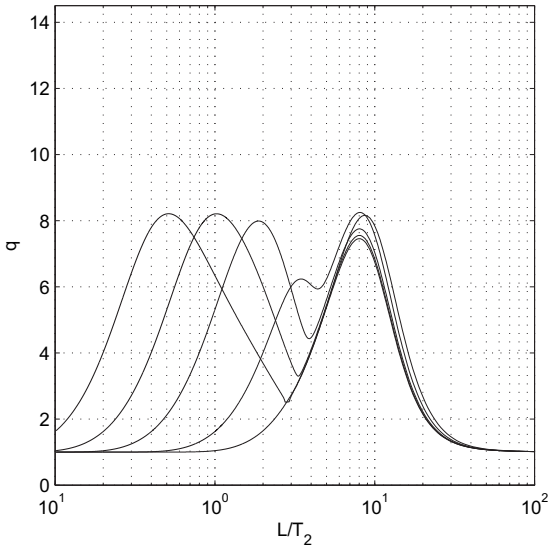

Fig. 7. Results for Model 2A series, a 5-layer multilayer with central thinner layer bounded by a finite soft layer ($T_1/T_2 = 3$) and a rigid frictionless platen. Viscosity ratio = 20. q spectra for different wavelengths, L (normalized to the outer stiff layer, T_2), where q is the dimensionless amplification factor; peaks signify dominant wavelengths (q_d, L_d) for single or multilayer folding. Curves are drawn for thin layer values, T_4/T_2, of 1.0, 0.5, 0.2, 0.1 and 0.05. The 1.0 curve has a single peak, not the maximum for this series. The 0.5 curve has a shoulder, and the 0.2, 0.1 and 0.05 curves have two peaks, right indicating ML mode and left SL mode which is only slightly stronger.

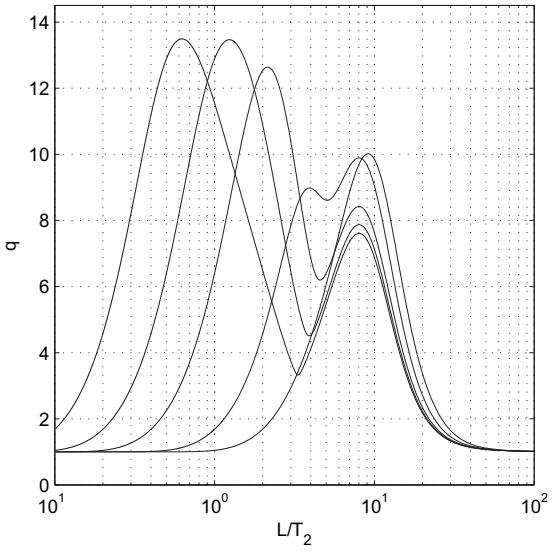

Fig. 8. Results for Model 2B series, a 5-layer multilayer with central thinner and stiffer layer bounded by a finite soft layer ($T_1/T_2 = 3$) and a rigid frictionless platen. Viscosity ratios 20 and 40. q spectra for different wavelengths, L (normalized to the outer stiff layer, T_2), where q is the dimensionless amplification factor; peaks signify dominant wavelengths (q_d, L_d) for single or multilayer folding. Curves are drawn for thin layer values, T_4/T_2, of 1.0, 0.5, 0.2, 0.1 and 0.05. The 1.0 curve has a single peak, not the maximum for this series. The 0.5 curve has a shoulder, and the 0.2, 0.1 and 0.05 curves have two peaks, right indicating a weak ML mode and left a very much stronger SL mode.

significant relative enhancement of the SL mode over the ML mode is achieved (Fig. 8), with q_d values of ~13.5 for SL and ~8 for ML folding, for $T_4/T_2 \leq 0.2$. Amplifications at 20% shortening are 13.5 and 5, and at 30% shortening, 49 and 11, for single-layer and multilayer folding, a significant difference. Compared to Model 1B (Fig. 6), which had the same layer variables but in a viscous half space, this SLU7 model with $T_1/T_2 = 3$ (Fig. 8) shows approximately the same SL q_d values for the central thin layer, but significantly lower ML q_d values for the multilayer mode, the effect of the confinement. Thus, in this model we see the greatest potential, so far, for developing stronger small-scale folding in one thin layer than the larger-scale folding of the whole multilayer: i.e. minor and major folds or parasitic folding.

In the next two models, we will specifically examine the effect of varying the thickness of the soft confining layers (T_1, T_7) against the rigid platens, on the folding of a multilayer with a thinner layer.

Model 2C is a variant of Model 2A, taking $T_4/T_2 = 0.2$ for the thinner middle layer, and now varying the thicknesses of the outer soft layers ($T_1 = T_7$) as $T_1/T_2 = 0.5, 1, 2, 3, 4$, to 10. All stiff layers have the same viscosity, and the stiff/soft ratio is 20, as in Model 2A. Fig. 9 shows the q spectra and L/T_2 values for this series. The common left peak is for 'single-layer' behaviour of the central stiff layer: note that there is no change with changing T_1. At $T_1/T_2 = 1$, the SL peak acquires a small satellite that represents a multilayer mode. As T_1/T_2 increases to 2, 3, 4, and 10, this peak increases, and between $T_1/T_2 = 3$ and 4, the multilayer peak becomes equal to the 'single-layer' peak, and for larger T_1/T_2, multilayer folding is the stronger mode. The maximum ML q_d for this model is ~10, where $T_1/T_2 = 10$, which is almost the same value as for the same multilayer in a viscous half space (Fig. 5).

Model 2D is essentially the same as Model 2C, except that the thin central layer is now twice as stiff. (It is a variant of Model 2B.) Fig. 10 shows the q spectra and L/T_2 values for this series. The model with $T_1/T_2 = 4$ is also shown in Fig. 4, used to illustrate the analytical method. The prominent central peak in Fig. 10 is, as before, that of

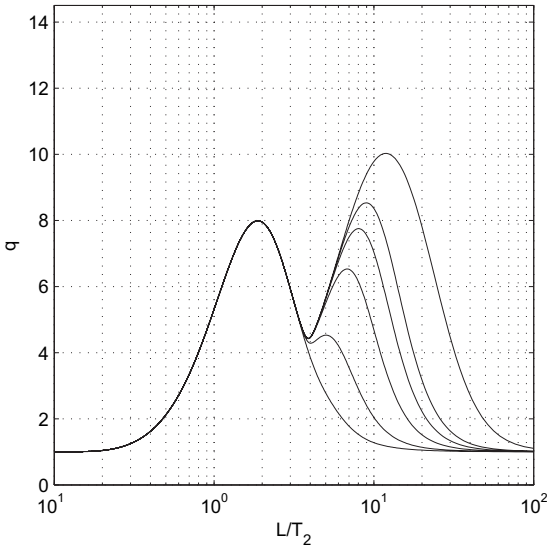

Fig. 9. Results for Model 2C series, a 5-layer multilayer with central thin layer with $T_4/T_2 = 0.2$, and variations in thickness of the bounding soft layer, T_1, against the RFP. Viscosity ratio = 20. q spectra for different wavelengths, L (normalized to the outer stiff layer, T_2), where q is the dimensionless amplification factor; peaks signify dominant wavelengths (q_d, L_d) for single or multilayer folding. Curves are drawn for $T_1/T_2 = 10$, 4, 3, 2, 1 and 0.5, decreasing downwards in the nested right-hand curves, with reducing values of ML q_d. The left peak is the SL mode, common to all the curves. The ML and SL modes have similar strengths when $T_1/T_2 = 3$–4.

the single-layer mode, the 'shoulder' for $T_1/T_2 = 1$ and the satellite peaks are for the multilayer mode. In all cases, from $T_1/T_2 = 0.5$ to 10, the q_d for the SL mode is measurably higher than for the ML mode. Thus, for all these models, we have stronger SL folding of the central layer than ML folding, which would produce small 'minor folds' on larger but weaker 'major folds'.

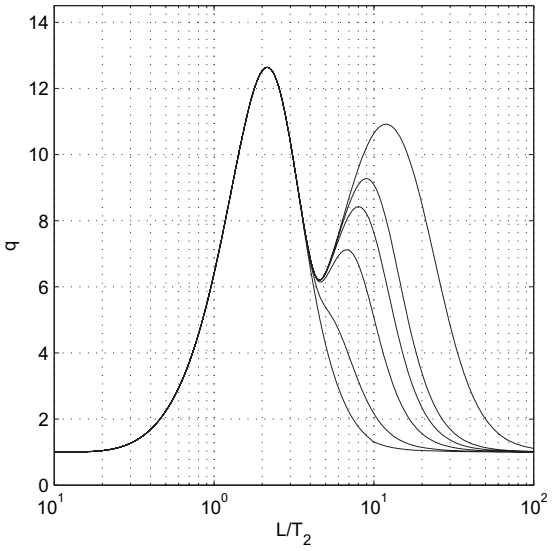

Fig. 10. Results for Model 2D series, a 5-layer multilayer with central thin and stiffer layer with $T_4/T_2 = 0.2$, and variations in thickness of the bounding soft layer, T_1, against the RFP. Viscosity ratios 20 and 40. q spectra for different wavelengths, L (normalized to the outer stiff layer, T_2), where q is the dimensionless amplification factor; peaks signify dominant wavelengths (q_d, L_d) for single or multilayer folding. Curves are drawn for $T_1/T_2 = 10$, 4, 3, 2, 1 and 0.5, decreasing downwards in the nested right-hand curves, with reducing values of ML q_d. The left peak is the SL mode, common to all the curves and the stronger mode in all these models.

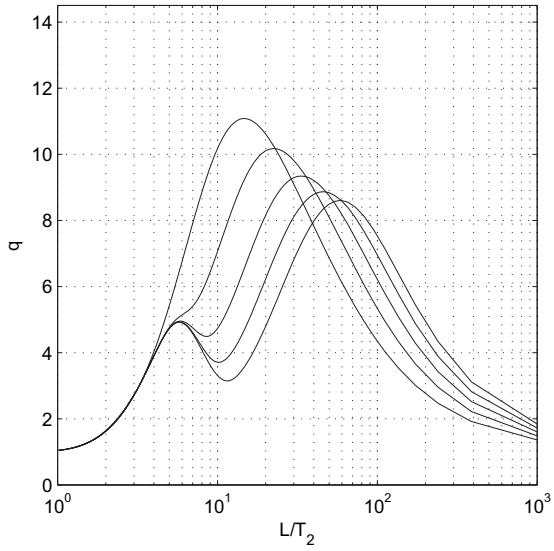

Fig. 11. Results for Model 3A series, a 5-layer multilayer with central thicker layer bound by a viscous half space. Viscosity ratio = 20. q spectra for different wavelengths, L (normalized to the outer stiff layer, T_2), where q is the dimensionless amplification factor; peaks signify dominant wavelengths (q_d, L_d) for single or multilayer folding. Curves are drawn for thick-layer values, T_4/T_2, of 1, 2, 3, 4, and 5, increasing downwards. Note the dominant ML mode with q_d values decreasing and L_d/T_2 values increasing with increasing T_4/T_2. Where present, the SL mode (lower left) is weak.

3.3. Model 3: 5-layer multilayer with central thick layer in viscous half space

This set of models complements the Model 1 set (Fig. 3a), with the same variables except that now we *increase* the thickness of the central stiff layer (T_4) so that $T_4/T_2 \geq 1$.

Model 3A comprises three stiff layers with thicknesses T_2, T_4 and T_6, separated by soft layers (T_3 and T_5), and bounded by viscous half space. The stiff/soft viscosity ratio is 20. All layer thicknesses (T_2, T_3, T_5, T_6) are the same, except for the central stiff layer (T_4), which is thicker, with values $T_4/T_2 = 1, 2, 3, 4$ and 5. Fig. 11 shows q spectra for the series of models, with wavelengths scaled to T_2. The highest peaks are for the ML mode, showing a maximum q_d for $T_4/T_2 = 1$, and progressively decreasing q_d and increasing L_d, as T_4/T_2 increases. Thus, as the thickness of the central stiff layer increases, rather than enhancing or 'controlling' multilayer folding, the opposite is found. The minor q peak at L/T_2 of ~ 6 that emerges for $T_4/T_2 > 1$ represents the weak single-layer mode for the outer (thinner) stiff layers. There are no circumstances in these models where single-layer folding could equal or exceed multilayer folding, in strength.

Model 3B is a series of experiments with the same variables as Model 3A, except that now we double the stiffness of the central thick layer, so that $\eta_4/\eta_3 = 40$, while $\eta_2/\eta_3 = 20$. As before, $T_3/T_2 = 1$ and $T_4/T_2 = 1$, 2, 3, 4 and 5. Fig. 12 shows q spectra for the series of models, with wavelengths scaled to T_2. The suite of peaks with $q_d = 13.2$–14.2 are for the ML mode, having L_d/T_2 values that increase as T_4/T_2 increases. As the thickness of the stiffest central layer (T_4) increases, there is only a slight decrease in ML q_d, compared to Model 3A (cf Fig. 11), but nevertheless the multilayer folding instability is strongest where $T_4/T_2 = 1$. The minor q peak at $L/T_2 \sim 6$ represents the weak single-layer mode for the outer (thinner) stiff layers, as in the previous model.

3.4. Model 4: 5-layer multilayer with central thick layer, in soft finite bounding layers against rigid frictionless platens: SLU7

This second SLU7 model is configured similarly to Model 2, Fig. 3(b), except that the central layer is thicker and we take

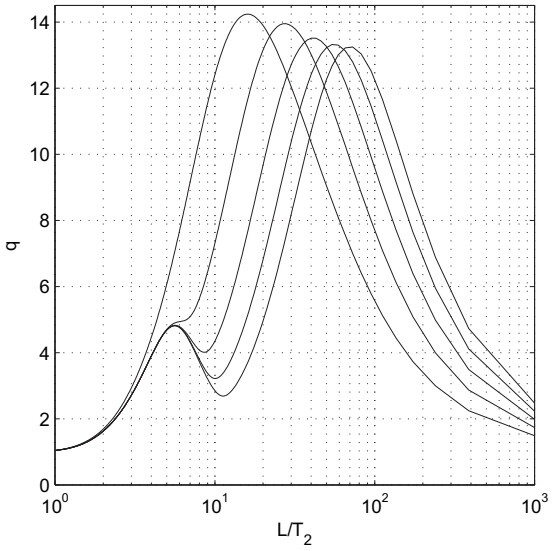

Fig. 12. Results for Model 3B series, a 5-layer multilayer with central thicker and stiffer layer bound by a viscous half space. Viscosity ratios 20 and 40. q spectra for different wavelengths, L (normalized to the outer stiff layer, T_2), where q is the dimensionless amplification factor; peaks signify dominant wavelengths (q_d, L_d) for single or multilayer folding. Curves are drawn for thick-layer values, T_4/T_2, of 1, 2, 3, 4, and 5, increasing downwards and rightwards. Note the dominant ML mode with q_d values decreasing and L_d/T_2 values increasing with increasing T_4/T_2. Where present, the SL mode (lower left) is weak.

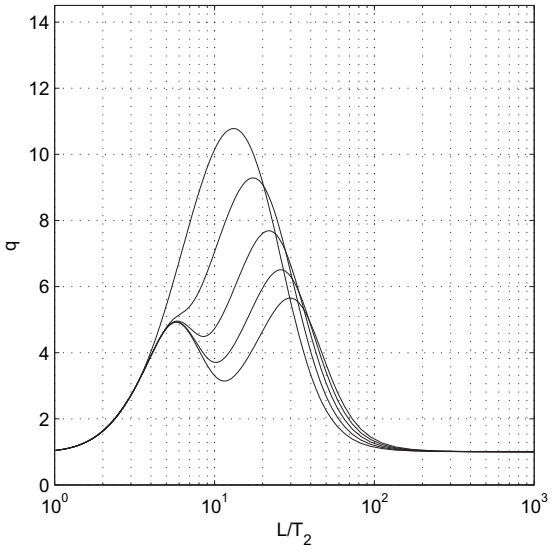

Fig. 13. Results for Model 4A series, a 5-layer multilayer with central thicker layer bounded by a finite soft layer ($T_1/T_2 = 10$) and rigid frictionless platens. Viscosity ratio = 20. q spectra for different wavelengths, L (normalized to the outer stiff layer, T_2), where q is the dimensionless amplification factor; peaks signify dominant wavelengths (q_d, L_d) for single or multilayer folding. Curves are drawn for thick-layer values, T_4/T_2, of 1, 2, 3, 4, and 5, increasing downwards. Note the dominant ML mode with q_d values decreasing and L_d/T_2 values increasing with increasing T_4/T_2. Where present, the SL mode (lower left) is weak.

$T_1/T_2 = 10$: i.e. the bounding soft layers are ten-times the thickness of the outer stiff layers. Model 4 otherwise uses the same variables as for Model 3, in order to examine the differences between multilayers embedded within a viscous half space, and those with a finite confinement.

Model 4A comprises three stiff layers with thicknesses T_2, T_4 and T_6, separated by soft layers (T_3 and T_5). These layer thicknesses (T_2, T_3, T_5, T_6) are all equal, except for the central stiff layer (T_4), which is thicker, with values $T_4/T_2 = 1$, 2, 3, 4 and 5. This 5-layer multilayer is bounded by soft layers ($T_1 = T_7$), with $T_1/T_2 = 10$. The stiff/soft viscosity ratio is 20. Fig. 13 shows q spectra for the series of models, with wavelengths scaled to T_2. The highest peak is for $T_4 = 1$, which is the pure multilayer mode. As T_4 increases, the ML q_d peaks significantly decrease, while the L_d/T_2 values increase. There is an approximate halving of the q_d as T_4/T_2 increases from 1 to 5. These results are a more exaggerated version of what was found for the viscous half space (Model 3A; Fig. 11), because of the increasing effect of the rigid platens as T_4 increases. The weaker peak that emerges with $L_d/T_2 \sim 6$ for $T_4/T_2 > 1$ is the SL mode for the outer stiff layers, as described for Fig. 11. This model with a finite confinement again demonstrates that the central thick layer does not 'control' or enhance multilayer buckling. However, for the thickest layer in our series, the SL mode for the outer layers is only slightly weaker than the ML mode, suggesting folds could grow simultaneously on different scales, $L_d/T_2 \sim 6$ and ~ 30.

Model 4B has all the same layer thickness properties as Model 4A, except that the viscosity ratio of the central thicker layer is now doubled to 40. The q spectra are shown in Fig. 14. Again, we see a significant drop in q_d for the ML mode, with increasing T_4; an approximate halving of value as T_4/T_2 changes from 1 to 5, signifying considerable dampening of the buckling instability. The weaker single-layer buckling mode has the same properties as described for Figs. 11–13, but in this series, remains always considerably weaker than even the weakest ML folding. We would therefore not expect to see fold growth on two scales, nor minor and major folds.

4. Discussion

There are many variables that are likely to control folding in multilayered viscous media and rocks. In this paper, we focus on conditions that could lead to simultaneous folding on different scales, such as a layer folding on a small scale within a multilayer that simultaneously folds on a larger scale, as depicted in Fig. 1. The

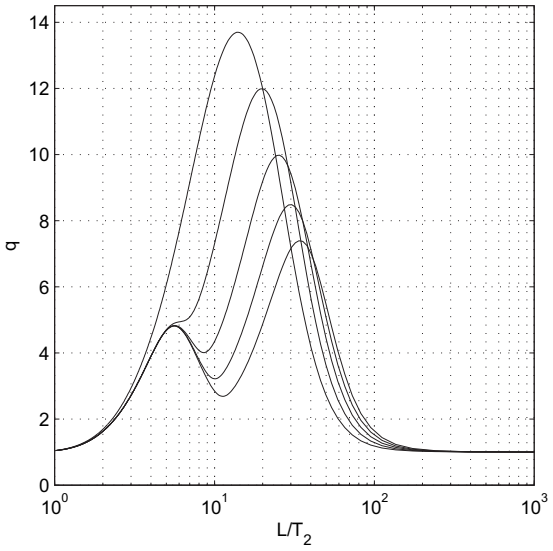

Fig. 14. Results for Model 4B series, a 5-layer multilayer with central thicker and stiffer layer bounded by a finite soft layer ($T_1/T_2 = 10$) and a rigid frictionless platen. Viscosity ratios 20 and 40. q spectra for different wavelengths, L (normalized to the outer stiff layer, T_2), where q is the dimensionless amplification factor; peaks signify dominant wavelengths (q_d, L_d) for single or multilayer folding. Curves are drawn for thick-layer values, T_4/T_2, of 1, 2, 3, 4, and 5, increasing downwards and rightwards. Note the dominant ML mode with q_d values decreasing and L_d/T_2 values increasing with increasing T_4/T_2. Where present, the SL mode (lower left) is weak.

chosen model is a 5-layer multilayer with alternating stiff (competent) and soft (incompetent) layers in bonded contact, with equal layer thicknesses except for the central stiff layer, which is thinner or thicker. These 5-layer multilayers are either confined in a semi-infinite soft medium (viscous half spaces), or within soft layers of finite thickness bounded by rigid frictionless platens to model a 'structural lithic unit' (Currie et al., 1962), a 7-layer unit we call SLU7. The only other variables in our models concern the central stiff layer: its thickness relative to the other layers, and its viscosity.

We use a stiff/soft viscosity ratio of 20 for one set of models, to represent the competence contrast during folding of competent and incompetent rocks. This is a compromise between the ratios of 50 or 100 usual for classical fold theory and modelling, and the lower ratios of <10 obtained from analyses of cleavage refraction and conglomerate deformation (Treagus, 1999; Treagus and Treagus, 2002). In the set of models where the thinner/thicker central layer is stiffer, this is modelled by doubling the viscosity of this layer so that the stiffer/soft ratio is 40 (a triple viscosity ratio of 40:20:1).

We will first discuss the models that comprise alternating stiff and soft layers with one viscosity ratio of 20. As noted in the Introduction, the type of multilayer that buckles with strongest instability and amplification is a bilaminate system of alternating stiff and soft layers with the same thickness, confined in a quasi-infinite soft medium (viscous half space). The greater the number of layers, and the higher the viscosity contrast, the greater the dominant fold amplification factor (q_d). This is confirmed in our first model, with Fig. 5 showing the maximum q peak for $T_4/T_2 = 1$ ($q_d = 11.1$, $L_d/T_2 = 14.5$). Such a model produces regular multilayer folds on one wavelength scale. However, where the same multilayer is in a finite and much narrower confining layer ($T_1/T_2 = 3$, Fig. 7), the maximum multilayer fold amplification is not when $T_4/T_2 = 1$. Although the differences are subtle, the greatest q value in Fig. 7 is when the central layer thickness is halved to $T_4/T_2 = 0.5$; we have $q_d = 8.25$, compared to $q_d = 8.16$ for $T_4/T_2 = 1$.

In this confined model (Fig. 7), when the central layer is even thinner ($T_4/T_2 \leq 0.2$), the q_d value for single-layer (SL) folding of the central thin layer slightly exceeds that for the whole multilayer (ML). Here, single and multilayer folds grow at almost the same rate, but on different scales. In models with $T_4/T_2 = 0.2$ and the confining layer thickness (T_1) is varied from $T_1/T_2 = 10$ to 0. 5 (Fig. 9), we are able to identify where single-layer folding of the thin layer amplifies more strongly than whole multilayer folding. The cross-over from stronger ML to SL folding is between T_1/T_2 of 3 and 4. Where $T_1/T_2 > 4$, ML folding prevails; where $T_1/T_2 < 2$, the ML mode is effectively suppressed and SL folding is dominant.

In models where the central thin layer is stiffer than the rest of the stiff layers (three-viscosity models with ratios 40:20:1), the results are somewhat different. This stiffening of just one layer has the effect of increasing the dominant amplifications and wavelengths of the multilayer and single-layer folding modes. For the viscous half space (Fig. 6), the ML mode has the strongest amplification of all when $T_4/T_2 = 1$, as found for the two-viscosity models, but now $q_d = 14.2$ and $L_d/T_2 = 16$. However, when $T_4/T_2 = 0.1$, the SL mode has notably higher q_d values than the ML mode (SL $q_d = 13.5$, ML $q_d = 10.2$), suggesting folding on two wavelength scales, the small SL folds amplifying more strongly than the larger ML folds. The results for the confined models with a stiffer and thinner central layer (Fig. 8) are similar, but the differences between the SL and ML q_d are even greater, because the confinement weakens the ML mode but hardly affects the SL mode. Thus, for $T_4/T_2 = 0.1$, we have SL $q_d = 13.5$ and ML $q_d = 8$.

For all the models with a much thinner central layer that is also stiffer, and especially when the multilayer is confined, small single-layer folds will grow more strongly than larger multilayer folds. These are the optimum conditions for producing folding on two scales, in a manner that would allow the smaller SL folds to be preserved as 'minor' folds around larger 'major' ML folds, as shown schematically in Fig. 1. This can now be improved on by our modelling. An example of two scales of folding is shown in Fig. 15, the two components representing local maximum growth rates determined by our analysis. The configuration is that of Model 2B (Figs. 3b and 8), with $T_4/T_2 = 0.2$. The lower figure shows the pair of components, equivalent to SL and ML modes, at sufficient amplitude to be visually distinct, and the upper figure shows the components after 10% additional layer-parallel shortening. Here, the reduction in wavelength with bulk shortening is not included. Although only the first-order analysis is used here, folds with such slopes would have reached the point where finite-amplitude effects would enter (see for example Johnson and Fletcher, 1994, section 5.5).

A subsidiary aim in this paper has been to test the proposal of Price and Cosgrove (1990), that anomalously thick competent layers in a multilayer act as 'control units' and dominate the folding. Accordingly, we also modelled 5-layer and 7-layer multilayers that had a thicker central stiff layer, either with the same or double the viscosity of the other stiff layers (Figs. 11–14). All the results here have shown that the multilayer buckling is not 'controlled' (in the sense of enhanced) by the thick layers. The opposite is seen, whether the multilayers are confined in a viscous half space or in finite confinement, and whether the central layer has the same or a greater viscosity as the other stiff layers. As the central (stiff) layer increases thickness, relative to the others, the maximum amplification factors (q_d) for multilayer folding decrease, while the wavelengths increase. For example, in the half space models (Fig. 11), $q_d = 11.1$ when $T_4/T_2 = 1$, but 8.6 when $T_4/T_2 = 5$. In all these thick-layer models, the single-layer mode q_d values (now for the relatively thinner outer stiff layers) are ~5, lower than the

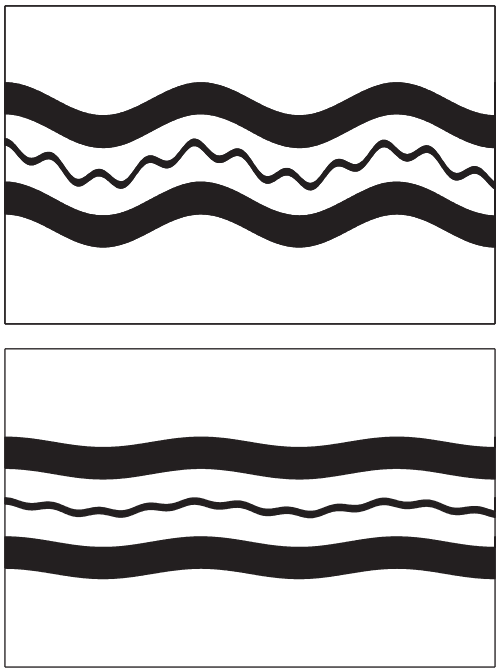

Fig. 15. Sum of a pair of multilayer folding components, here the low-amplitude eigenmodes at wavelengths for two peaks in the q-spectrum (SL and ML). The lower figure shows visually distinct low-amplitude folding, and the upper figure after 10% additional layer-parallel shortening. The layer configuration is that of Model 2B (Fig. 8), with $T_4/T_2 = 0.2$ and a central stiff layer having twice the viscosity of the symmetrically disposed stiff layers. Viscosity ratios 20 and 40.

multilayer values in all cases, all the more so when the central layer is stiffer (Fig. 14). Only one experiment (Model 4A, Fig. 13), where $T_4/T_2 = 5$ (the thickest example), indicated the potential for weak folding with similar amplification, on two scales. For all the rest, we deduce that folds will develop and grow on only one scale, that of the whole multilayer.

We now discuss these results in terms of multilayer folding in rocks, and questions posed in the Introduction: such as why small-scale 'minor' folds develop and are preserved in larger-scale 'major' folds, when it is known that a stack of many layers should fold more strongly than a single layer. Stratified rocks are unlikely to be regular alternations of competent and incompetent rocks with identical thicknesses and just two effective viscosities; nor will multilayered rocks be always confined in an incompetent medium that can be approximated to infinite or a 'half space'. Our models have simple designs to test some existing concepts, and to seek parameters that might 'control' multilayer folding on different scales, as is seen in real fold belts. The models are relevant to folding of rocks with irregular alternations of two or three lithologies, such as limestone/sandstone/mudstone, or quartzite/psammite/pelite sequences.

The results suggest that an unusually *thin competent bed*, especially if somewhat more competent than other competent beds, can fold more strongly than the multilayer stack, to develop the classic structural features of minor and major folds idealised in Fig. 1. For example, a thin quartzite within a layered psammite/pelite sequence should initiate the strongest folds, taking on the classic asymmetric geometry of minor folds around major folds as they become involved in larger-scale but weaker multilayer folding (Fig. 1). In other cases, multilayer folding, whether of a whole sequence of competent and incompetent rocks, or packets (structural lithic units, Currie et al., 1962) within it, may develop on several different scales that have similar growth rates, with overlapping or interfering wavelengths. Our results broadly support Ramberg's (1962) 'zone of contact strain' that is approximately one fold wavelength deep; e.g. in Fig. 5, single-layer folding parameters stabilise at $T_3/T_2 = T_4/T_2 = 0.1$, i.e. where SL $L/T = 10$. However, in practice, the middle thin layers in our models appear to behave as approximate single layers when the surrounding soft layer is $\sim$0.8 times the SL wavelength.

Small-scale or single-layer folds that would potentially initiate with a much smaller amplification factor than the larger multilayer folds, are unlikely to grow successfully. Instead, they will be carried by the multilayer folding into larger wavelengths folds. Small folds that have developed to finite scale within larger fold structures, such as those used by structural geologists to map larger-scale structures, must have initiated with a stronger amplification than the multilayer folds.

Finally, what is the significance of an unusually *thick competent bed* in the folding of multilayered rocks? This, it was suggested (Price and Cosgrove, 1990), would act effectively as a single-layer 'control unit' within the multilayer, that would dominate folding. Our models show the opposite: that an anomalously thick stiff layer will not fold as a 'single layer' to enhance folding, but will impede multilayer folding, with each increase in thickness reducing the amplification factor for the dominant ML wavelength (Figs. 11–14). These effects are particularly significant for a finitely confined multilayer, which is probably the more geologically relevant.

Given the discussion above regarding the role of thinner (and perhaps stiffer) competent layers, and the required thickness of adjacent incompetent layers to allow these layers to fold as independent single layers, we suggest that unusually thick incompetent layers might have a more significant control on multilayer folding than unusually thick competent layers. This appears to be borne out by our field observations on a small scale, and is being followed up in further work.

5. Conclusions

In multilayers that are not made up of exactly equal thicknesses of stiff/competent and soft/incompetent layers, folds can develop and grow simultaneously on different scales. To develop small folds around larger folds, with the characteristic changes of symmetry and vergence of minor folds on major folds used by field geologists, the small folds must have grown at a greater amplification rate than the larger folds. Our viscous multilayer models with a central thinner layer demonstrate that folds in the thin layer will initiate with greater amplification than larger folds of the whole multilayer, if the multilayer is narrowly confined, and/or if the thin layer is the stiffest layer. Folds will develop on two scales, creating 'minor' and 'major' folds.

In multilayer models where the central stiff layer is thicker than the others, we find that the strength of multilayer folding is progressively reduced, as the layer thickness increases. Unusually thick competent layers in a multilayer therefore cannot be said to control the folding, or act as 'control units' in a multilayer; they will actually impede the folding.

Acknowledgements

SHT thanks the convenors at GSA Seattle (2003) for the invitation to talk about relationships of stratigraphy, lithology and folding, which rekindled her interest in folding of rocks. SHT acknowledges funding of a Senior Research Fellowship from NERC that provided support at the start of the work, to SEAES Manchester University for supporting her current position, to Dave Pollard for enabling us to present this work at GSA Houston (2008), and to SEAES for providing support for her attendance. RCF was supported by a Centre of Excellence grant from the Norwegian Research Council to PGP. We thank the reviewers, Bruce Hobbs and Stefan Schmalholz, for their comments which helped us clarify this paper.

References

Biot, M.A., 1961. Theory of folding of stratified viscoelastic media and its implications in tectonics and orogenesis. Geological Society of America Bulletin 72, 1595–1620.
Biot, M.A., 1965a. Theory of similar folding of the first and second kind. Geological Society of America Bulletin 76, 251–258.
Biot, M.A., 1965b. Mechanics of Incremental Deformations. John Wiley and Sons, New York.
Currie, J.B., Patnode, H.W., Trump, R.P., 1962. Development of folds in sedimentary strata. Geological Society of America Bulletin 73, 655–674.
Frehner, M., Schmalholz, S.M., 2006. Numerical simulations of parasitic folding in multilayers. Journal of Structural Geology 28, 1647–1657.
Johnson, A.M., Fletcher, R.C., 1994. Folding of Viscous Layers. Columbia University Press, New York.
Mühlhaus, H.-B., Moresi, L., Hobbs, B., Dufour, F., 2002. Large amplitude folding in finely layered viscoelastic rock structures. Pure and Applied Geophysics 159, 2311–2333.
Price, N.J., Cosgrove, J.W., 1990. Analysis of Geological Structures. Cambridge University Press, Great Britain.
Ramberg, H., 1962. Contact strain and folding instability of a multilayered body under compression. Geologische Rundshau 51, 405–439.
Ramberg, H., 1963. Fluid dynamics of viscous buckling applicable to folding of layered rocks. Bulletin of the American Association of Petroleum Geologists 47, 484–505.
Ramberg, H., 1964. Selective buckling of composite layers with contrasted rheological properties, a theory for the simultaneous formation of several orders of folds. Tectonophysics 1, 307–341.
Sherwin, J.-A., Chapple, W.M., 1968. Wavelengths of single layer folds: a comparison between theory and observation. American Journal of Science 266, 167–179.
Schmid, D.W., Podladchikov, Y.Y., 2006. Fold amplification rates and dominant wavelength selection in multilayer stacks. Philosophical Magazine 86, 3409–3423.
Treagus, S.H., 1999. Are viscosity ratios of rocks measurable from cleavage refraction? Journal of Structural Geology 20, 895–901.
Treagus, S.H., Treagus, J.E., 2002. Studies of strain and rheology of conglomerates. Journal of Structural Geology 24, 1541–1567.